$^{16}O^{13}C^{18}O$: high-resolution absorption spectrum between 4000 and 9500 cm^{-1} and global fitting of vibration–rotational line positions[☆]

Y. Ding,[a] V.I. Perevalov,[b] S.A. Tashkun,[b] J.-L. Teffo,[c] A.-W. Liu,[a] and S.-M. Hu[a,*]

[a] *Laboratory of Bond Selective Chemistry, Department of Chemical Physics, University of Science and Technology of China, Hefei, 230026, People's Republic of China*
[b] *Institute of Atmospheric Optics SB RAN, 1, Akademicheskii av., 634055 Tomsk, Russia*
[c] *Laboratoire de Physique Moléculaire et Applications (Unité mixte C.N.R.S/Université Pierre et Marie Curie), Case Courrier 76, Université Pierre et Marie Curie, 4 Place Jussieu, 75252 Paris Cedex 05, France*

Received 4 June 2003; in revised form 29 July 2003

Abstract

The absorption spectrum of a ^{13}C enriched carbon dioxide sample has been recorded with a Fourier-transform spectrometer in the spectral range 4000–9500 cm^{-1}. In addition to six bands observed from the spectrum of the atmosphere of Venus in this region, eight new $^{16}O^{13}C^{18}O$ bands were measured. The new observations together with the data collected from the literature have been used to fit parameters of an effective Hamiltonian for the $^{16}O^{13}C^{18}O$. More than 4000 line positions in 38 bands have been used to derive 48 parameters of effective Hamiltonian. The RMS (root-mean-square of residuals) of the fit is 0.00106 cm^{-1}.
© 2003 Elsevier Inc. All rights reserved.

1. Introduction

Carbon dioxide is a trace gas in the terrestrial atmosphere. It is produced by industrial and domestic combustion, space and aircraft vehicle exhaust and plays an important role in the green-house effect and planetary atmosphere. Its strong opacity in the infrared has a major impact on the environment and it is often a contaminant in infrared spectra. Due to its importance, CO_2 is one of the most investigated molecules from the spectroscopic point of view [1]. However, there remains a need for the investigation of additional vibrational and rotational levels. The present study is devoted to the asymmetric isotopic species $^{16}O^{13}C^{18}O$ of the carbon dioxide molecule. As for natural abundance this species is the fifth after $^{12}C^{16}O_2$, $^{13}C^{16}O_2$, $^{16}O^{12}C^{18}O$, and $^{16}O^{12}C^{17}O$. Several previous studies have been reported [2–14]. But all these works focused on the region less than 4000 cm^{-1}. In the higher spectral region, only Venus spectra were reported. The first Venus spectrum were recorded by Connes in 1966 with the resolution 0.1 cm^{-1} and interpreted in [15]. In 1973 Connes and Michel [16] obtained a higher resolution (0.015 cm^{-1}) spectrum of the atmosphere of Venus. In 1977 Mandin [17] presented the analysis of these data. We are also aware of unpublished results of Miller [18] in the spectral region higher than 4000 cm^{-1}. In this work, the high-resolution absorption spectrum of $^{16}O^{13}C^{18}O$ was recorded between 4000 and 9500 cm^{-1}. Overall 11 cold and 3 hot bands have been analyzed. Among them 6 bands were reported previously by Mandin [17].

The observed line positions together with those collected from literature [2–14,17] have been used to derive parameters of the reduced effective Hamiltonian, which has been developed in [19] and successfully applied for the global treatment of the vibration–rotational energy levels of $^{12}C^{16}O_2$ [20], $^{13}C^{16}O_2$ [21], $^{16}O^{12}C^{18}O$, and $^{16}O^{12}C^{17}O$ [22]. In the last section of the paper we give also the comparison of observed data with those presented in HITRAN [23] for the $^{16}O^{13}C^{18}O$ isotopic species.

2. Experimental details

The absorption spectra of a carbon dioxide sample enriched with ^{13}C have been recorded in the spectral range from 4000 to 9500 cm^{-1} with a Bruker IFS 120HR Fourier-transform spectrometer (FTS) equipped with a path length adjustable multi-pass gas cell. The maximum optical path length is 105 m. The sample was purchased from Aldrich Chemical. The stated isotopic concentration is 99% of ^{13}C for carbon atom and 6% of ^{18}O for oxygen atom. A mass spectroscopy experiment has given the following isotopic abundance in the sample: $^{13}C^{16}O_2$ 95.3%, $^{16}O^{13}C^{18}O$ 2.4%, $^{12}C^{16}O_2$ 1.8%, and $^{16}O^{13}C^{17}O$ 0.5%. Because of the wide spectral range and the large variation of the absorption line intensities, different experimental conditions were used as listed in Table 1. A tungsten source, CaF$_2$ beam splitter were used in all experiments. Parts of spectra are presented in Figs. 1 and 2. The line positions were calibrated using those of $^{12}C^{16}O_2$ listed in HITRAN-96 database [23]. The accuracy of line positions of unblended and not-very-weak lines was estimated to be better than 0.001 cm^{-1}.

3. Rotational analysis and vibrational assignment

The standard expression were used for the vibration–rotational energy levels of the upper and lower states

$$T_v = G_v(v_1, v_2^{l_2}, v_3) + F_v(J), \tag{1}$$

where G_v and F_v are the vibrational and rotational contributions, respectively, with

$$F_v(J) = B_v[J(J+1) - K^2] - D_v[J(J+1) - K^2]^2, \tag{2}$$

where $K = l_2$ is the quantum number associated to the vibrational angular momentum.

In the fitting procedure the rotational constants of the ground state, B'' and D'', were constrained to their literature values [1] and the quantities v_0, ΔB, and ΔD were fitted. On the basis of combination differences, 11 cold bands and 3 hot bands can be assigned to the $^{16}O^{13}C^{18}O$ species. Rotational levels with J value up to 61 have been assigned. The spectroscopic parameters retrieved
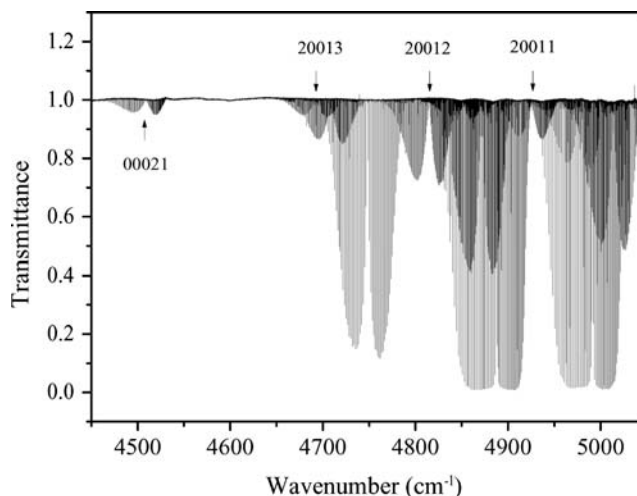

Fig. 1. Overview of the absorption spectrum of ^{13}C enriched carbon dioxide sample between 4450 and 5050 cm^{-1}. Some $^{13}C^{16}O_2$ bands are saturated. Bands of $^{16}O^{13}C^{18}O$ isotope are marked in the figure. Spectrum is recorded with resolution 0.005 cm^{-1}, InSb detector, total gas pressure 1089 Pa, and absorption path length 15 m.
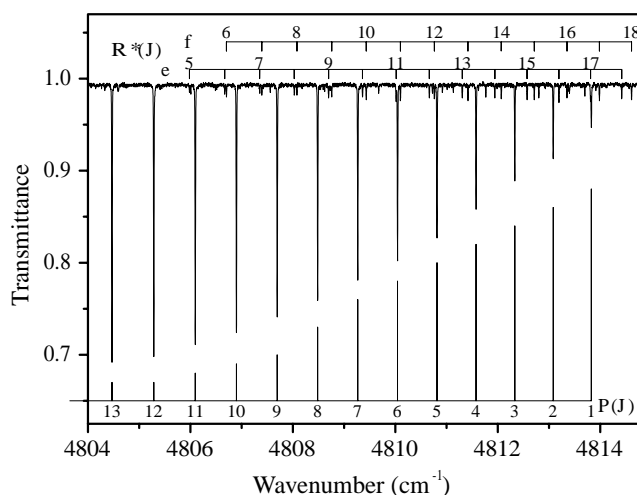

Fig. 2. $^{16}O^{13}C^{18}O$ spectrum in the part of the P-branch of the strong Σ–Σ band centered at 4814.5627 cm^{-1}. This band is superimposed with R-branch $R*(J)$ of the weak Π–Π hot band centered at 4801.6945 cm^{-1}. The experimental condition is the same as shown in Fig. 1.

Table 1
Experimental conditions used to record the Fourier-transform absorption spectra of ^{13}C enriched carbon dioxide

Region (cm^{-1})	Gas pressure[a] (Pa)	Detector	Length of absorption path (m)	Resolution (cm^{-1})
4400–5050	50.2	InSb[b]	15	0.005
4400–5050	1089	InSb[b]	15	0.005
4400–7600	2433	InSb[b]	69	0.01
5500–9500	3213	Ge	105	0.01
6000–8000	389	InSb[b]	15	0.007

[a] Total pressure. The concentration of $^{16}O^{13}C^{18}O$ in our sample is around 2.4%.

[b] Liquid-nitrogen cooled.

from the fitting of the energy levels are presented in Tables 2 and 3 for the cold and hot bands, respectively. Here the vibrational levels are labeled using the HITRAN notation [1]. The RMS deviations are less than $0.001 \, \text{cm}^{-1}$ for not very weak bands, close to the experimental uncertainty, and slightly larger (about $0.002 \, \text{cm}^{-1}$) for the weak bands. Full list of the assigned rotational lines are available as supplementary data attached to the paper.

Six cold bands in this region were previously reported by Mandin [17]. As a comparison, his spectroscopic parameters are also listed in italics in Table 2. They are in good agreement with our measurements. Due to the higher resolution and less impurity of gas sample, more rotational transitions are observed in our experiment and lead to probably more reliable parameter values. The improvement of the rotational parameters is very prominent for the 20012 and 20011 states. For these states the

parameters derived from the Venus spectra gave very large RMS values. Transitions belonging to three bands (20013–00001, 20012–00001, and 20011–00001) are listed in the HITRAN-96 database [23]. Our observed line positions of the 20013–00001 band are close to those listed in HITRAN (differences are less than $0.001 \, \text{cm}^{-1}$). For the other two bands large differences between observed and HITRAN line positions can be seen. For example, the deviation increases from 0.003 to $0.05 \, \text{cm}^{-1}$ when the J value increases from 4 up to 32 for the 20011–00001 band.

The vibrational assignment of newly observed bands is straightforward. It has been performed using predictions with the help of the effective Hamiltonian presented in our previous paper [19], which was developed on the basis of the effective Hamiltonian used by Chedin [24]. The preliminary set of effective Hamiltonian parameters has been obtained by fitting to the observed line positions collected from the literature [2–14,17].

Table 2
Spectroscopic parameters (in cm^{-1}) for the Σ levels of $^{16}O^{13}C^{18}O$ observed in this work

$^{16}O^{13}C^{18}O$	G_v	B_v	$D_v \times 10^7$	J_{MAX} P/R	n/N[b]	rms ($\times 10^4$)
Ground state[a]	0.0	0.36818116	1.18498			
00021	4508.74747(8)	0.36260285(16)	1.17914(53)	57/56	114/114	4.7
	4508.7479(1)	*0.3626082 (4)*	*1.205(2)*			*4.8*
20013	4692.17902(10)	0.36650356(19)	1.59678(63)	58/55	104/108	5.3
	4692.1792(3)	*0.3665110(13)*	*1.642(9)*			*13.9*
20012	4814.56272(13)	0.36483787(20)	1.22757(56)	65/61	120/123	7.7
	4814.5708(84)	*0.364816(30)*	*1.00 (21)*			*142*
20011	4925.01823(6)	0.36550368(15)	0.85377(73)	50/47	89/91	3.0
	4925.0084(70)	*0.365557(38)*	*1.91(33)*			*164*
10022	5712.61122(43)	0.3631215(19)	1.325(15)	30/35	46/58	13.6
10021	5809.86184(27)	0.3623583(11)	1.0067(86)	37/38	64/76	10.1
30013	6026.62451(15)	0.36517445(44)	1.5462(23)	47/45	87/90	7.4
	6026.6282(8)	*0.3651672(79)*	*1.41(14)*			*18.3*
30012	6140.12291(16)	0.36453200 (43)	0.87837(22)	45/46	84/86	7.3
30011	6279.48825(51)	0.3659154(21)	0.686 (16)	22/36	36/46	14.0
00031	6728.35464(9)	0.35981671(17)	1.17846 (65)	57/43	87/94	4.3
	6728.3586(6)	*0.3598217(14)*	*1.206(13)*			*7.0*
10031	8009.25536 (69)	0.3595215(24)	1.009(17)	37/38	48/65	20.5

Note. The uncertainties are given in parenthesis in the unit of the last quoted digit. The parameters in italics listed are the results of Mandin [17]. The contribution from H_v is neglected.
[a] The parameters for the ground level are taken from [1].
[b] n, number of transitions included in the fit; N, number of assigned rotational transitions.

Table 3
Spectroscopic parameters (in cm^{-1}) for the Π–Π hot bands of $^{16}O^{13}C^{18}O$ observed in this work

$^{16}O^{13}C^{18}O$	v_0[b]	B_v	$D_v \times 10^7$	J_{MAX} P/R	N/N[c]	rms ($\times 10^4$)
01101e[a]		0.36856153	1.20496			
01101f[a]		0.36911244	1.20134			
01121e–01101e	4485.59097 (63)	0.3630386 (24)	1.201 (18)	37/37	25/63	10.3
01121f–01101f	4485.59119 (55)	0.3635532 (24)	1.160 (22)	36/37	24/63	8.0
21113e–01101e	4649.92417 (29)	0.3662961 (12)	1.1505 (95)	37/37	58/69	9.8
21113f–01101f	4649.92490 (29)	0.3676167 (11)	1.5372 (77)	37/39	63/72	7.5
21112e–01101e	4801.69313 (58)	0.3652022 (17)	0.9938 (91)	44/40	62/77	17.0
21112f–01101f	4801.69590 (59)	0.3661949 (19)	0.951 (11)	42/40	66/79	20.2

Note. The uncertainties are given in parenthesis in the unit of the last quoted digit.
[a] The parameters for the lower states are taken from [1].
[b] Band origin. The corresponding vibrational term values of the 01121, 21113, and 21112 are 5128.9145, 5293.2515, and 5445.0204 cm^{-1}, respectively.
[c] n, number of transitions included in the fit; N, number of assigned rotational transitions.

4. Global fitting of vibration–rotational line positions

The line positions of the newly observed bands have been added to the input data. The total number of collected observed wavenumbers was 4388. The first stage of the fitting is the analysis of the internal consistency of the used data from the point of view of the assignment, possible measurement errors, misprints of published line positions and recovering probable calibration factors, and averaged pressure shifts of various spectra relative to each other. As in our previous papers [21,22], we have used the fundamental Ritz principle for this purpose. a brief outline of this approach is given below. To account for the possible calibration factors and pressure shifts, the Ritz principle can be written in the form

$$(1 + \delta^k)v_{j \leftarrow i}^k = E_j - E_i,\qquad(3)$$

where $v_{j \leftarrow i}^k$ is the observed line position belonging to the kth spectrum, i and j are composite indexes of the relevant quantum numbers which define the spectroscopic assignment of the observed transition, δ^k is the calibration offset for this spectrum, and E_i and E_j are the energies (term values) of the lower and upper states, respectively. The calibration factor for the kth spectrum is $(1 + \delta^k)$. Eqs. (3) with the different indexes i, j, and k constitute the overdetermined system of linear equations. The quantities δ^k are set to zero for some reference spectra (e.g., the microwave measurements and laser heterodyne measurements) and are considered as unknowns for the other type spectra. Many measured FTS spectra contain wavenumbers for several species. The probable calibration offset for a spectrum of this type is recovered using wavenumbers of the most abundant species. Then this factor is used as the fixed input value of δ^k for this spectrum when considering the next abundant species, etc. This approach enables us to recover calibration factors in the most reliable way. The solution of the system (3) in the least-squares sense is

equivalent to minimizing the dimensionless weighted standard deviation

$$\chi_{\mathrm{RITZ}} = \sqrt{\frac{\sum[((1 + \delta^k)v_{j \leftarrow i}^k - E_j + E_i)/\varepsilon^k]^2}{N_{tra} - N}},\qquad(4)$$

where summation goes over all transitions included into a datafile, ε^k is the experimental uncertainty of the kth spectrum, N is the number of unknowns and N_{tra} is the number of the transitions in the datafile. It is worth pointing out a wrong definition of χ_{RITZ} given in [22], in which the factor $(1 + \delta^k)$ has been missed. The value of χ_{RITZ} provides a measure of total consistency of observed wavenumbers in the datafile. It should be stressed that this value is independent of any Hamiltonian model and is calculated from the first principles of the quantum mechanics only. The values of the individual residuals

$$r_{j \leftarrow i} = (1 + \delta^k)v_{j \leftarrow i}^k - (E_j - E_i)\qquad(5)$$

enable us to detect outliers, i.e., misprints, misassignments or badly measured wavenumbers. The value of

$$RMS_{\mathrm{RITZ}} = \sqrt{\frac{1}{N_{tra}} \sum \left[(1 + \delta^k)v_{j \leftarrow i}^k - E_j + E_i\right]^2}\qquad(6)$$

gives the lower bound for the RMS when a Hamiltonian model is used. The values of RMS_{RITZ} deviation for each spectrum provide an estimate of the *actual* average experimental precision. Finally, after solving the system of Eqs. (3) we have a set of *experimental* energy levels $\{E_i\}$ of a species derived from observed transition frequencies.

After removing 200 outliers having large residuals the file of input data contained 4188 observed line positions. The solution of the system of linear equations in a least-squares sense with respect to energy levels and calibration factors gave $\chi_{\mathrm{RITZ}} = 1.52$ and $RMS_{\mathrm{RITZ}} = 0.0007\,\mathrm{cm}^{-1}$. The source-by-source characteristics of the input data are given in Table 4. They include, for each source, the calibration factors, experimental

Table 4
Experimental data and statistics of the line positions fit for $^{16}O^{13}C^{18}O$ (spectrum-by-spectrum analysis)

Reference	Calibration factor	Precision (in $10^{-3}\,\mathrm{cm}^{-1}$)	N_{fit}[c]	RMS_{RITZ} (in $10^{-3}\,\mathrm{cm}^{-1}$)	RMS_{GIP} (in $10^{-3}\,\mathrm{cm}^{-1}$)
Bradley et al. [13]	1.000000000	0.001	76	0.005	0.015
Jolma [9]	1.000000000	0.04	335	0.17	0.26
Toth [10]	0.999999761[a]	0.10	46	0.23	0.28
Bailly and Rossetti [14]	0.999999689	0.50[b]	752	0.20	0.42
Esplin et al. [4–7]	0.999999626[a]	0.40	735	0.54	1.45
Esplin and Hoke [8]	1.000000000[a]	0.50	884	0.85	1.01
Malathy Devi et al. [11]	1.000000071[a]	0.50[b]	19	0.24	1.38
Rinsland et al. [12]	1.000000054[a]	0.50[b]	14	0.00	1.43
Our data	0.999999828	1.00	1130	0.60	1.21
Baldacci et al. [2]	1.000000000[a]	3.00	40	1.09	1.07
Baldacci et al. [3]	1.000000000[a]	5.00	31	2.24	2.09
Mandin [17]	0.999999442[a]	2.00[b]	125	1.81	1.87

[a] Calibration factor is fixed to the value from [21,22].
[b] Experimental precision is set to a guessed value.
[c] N_{fit} is the number of lines included in the fit.

Table 5
Effective Hamiltonian parameters for $^{16}O^{13}C^{18}O$

N	Parameter	Value (cm^{-1})	Order
Diagonal vibrational parameters			
1	ω_1	1314.3236(30)	
2	ω_2	648.4462(11)	
3	ω_3	2309.80274(64)	
4	x_{11}	−2.70220(56)	
5	x_{12}	−4.6273(39)	
6	x_{13}	−17.8952(21)	
7	x_{22}	1.44577(76)	
8	x_{23}	−11.61774(90)	
9	x_{33}	−11.65269(16)	
10	x_{ll}[a]	−0.939752927	
11	y_{113}	−8.495(27)	10^{-2}
12	y_{122}	−3.795(13)	10^{-2}
13	y_{123}	−9.34(55)	10^{-2}
14	y_{133}	5.281(22)	10^{-2}
15	y_{222}[a]	−0.4203561690	10^{-2}
16	y_{223}	1.92(10)	10^{-2}
17	y_{233}	1.2735(70)	10^{-2}
18	y_{333}	0.2685(24)	10^{-2}
19	y_{1ll}[a]	5.582148965	10^{-2}
20	y_{2ll}	1.124(18)	10^{-2}
21	y_{3ll}	−1.28(10)	10^{-2}
22	z_{3333}	0.2349(16)	10^{-3}
Diagonal rotational and vibrational–rotational parameters			
23	B_e	0.36948188(15)	
24	α_1	1.08971(19)	10^{-3}
25	α_2	−0.669520(97)	10^{-3}
26	α_3	2.81048(19)	10^{-3}
27	γ_{11}[a]	−0.1469432390	10^{-5}
28	γ_{12}[a]	1.043729480	10^{-5}
29	γ_{13}	−5.982(35)	10^{-5}
30	γ_{22}	−0.3822(17)	10^{-5}
31	γ_{23}	−1.197(17)D	10^{-5}
32	γ_{33}	0.1208(54)	10^{-5}
33	D_e	0.116865(35)	10^{-6}
34	β_1	−0.168(28)	10^{-9}
35	β_2	2.0066(79)	10^{-9}
36	β_3	−0.3053(99)	10^{-9}
37	H[a]	0.7504935530	10^{-14}
Parameters of l—doubling matrix elements			
38	L_e	−0.141093(49)	10^{-3}
39	L_1[a]	0.4591757370	10^{-6}
40	L_2	2.171(24)	10^{-6}
41	L_3	−11.220(78)	10^{-6}
42	L_J	0.1776(33)E	10^{-9}
Parameters of Fermi-interaction matrix elements			
43	F_e	−25.24465(52)	
44	F_1	0.25627(18)	
45	F_2	0.29856(32)	
46	F_3	0.14343(17)	
47	F_{12}	−0.5045(97)	10^{-2}
48	F_{33}	−0.625(13)	10^{-2}
49	F_j	0.107611(31)	10^{-3}
50	F_L	−0.9491(59)	10^{-5}
51	F_e^{IV}[a]	0.1648736709	10^{-1}
Parameters of Coriolis-interaction matrix elements			
52	C_e	−0.7086(20)	10^{-1}
53	C_1[a]	0.2767539120	10^{-3}
54	C_2	1.579(19)	10^{-3}
55	C_3	−0.612(32)	10^{-3}

Table 5 (continued)

N	Parameter	Value (cm^{-1})	Order
56	C_l[a]	0.4826858884	10^{-3}
57	C_J	0.2375(46)	10^{-6}
58	C_{e2}	1.0077(83)	10^{-2}

Note. Uncertainties in parentheses represent one standard deviation in units of the last quoted digit.
[a] Fixed to the value given in [24].

uncertainties, and weighted standard deviations χ_{RITZ}. The majority of the collected line positions originate from spectra that contain also the line positions of the more abundant isotopic species $^{12}C^{16}O_2$, $^{13}C^{16}O_2$, $^{16}O^{12}C^{18}O$, and $^{16}O^{12}C^{17}O$. The corresponding calibration factors for these spectra were taken from our previous papers [21,22] and are used in the present work as fixed values. They are marked with an [a] in Table 4. The calibration offset for the high-precision laser heterodyne measurements [13] was fixed to zero. The experimental uncertainties have been taken from the corresponding papers. They are given in Table 4 in the column named "Precision." Sometimes there is no explicit indication of the uncertainties of the observed line positions. In this case we used guessed values which are marked with the [b] symbol. For our new measured data $RMS_{RITZ} = 0.0006\ cm^{-1}$. This value can be considered as the actual average experimental precision of these data.

As in our previous papers [20–22] the least-squares fits of the effective Hamiltonian parameters to the observed line positions have been performed with the help of the GIP computer code [25]. The aim of the fitting procedure was to minimize the dimensionless weighted standard deviation defined according to the usual formula

$$\chi_{GIP} = \sqrt{\frac{\sum_i \left[(v_i^{obs} - v_i^{calc})/\varepsilon^k\right]^2}{N - n}}, \qquad (7)$$

where N is the number of fitted transitions, n is the number of adjusted parameters, and ε^k is the experimental uncertainty of the kth spectrum. The values of the parameters published by Chédin [24] were used as initial guess. For the sake of the effective Hamiltonian reduction three parameters have been fixed to the values given in [24]: $x_{ll} = -0.939752927\ cm^{-1}$, $y_{1ll} = 0.05582148965\ cm^{-1}$, and $y_{222} = -0.004203561690\ cm^{-1}$. In the process of fitting it was found reasonable to fix in addition 7 other parameters to the values reported in [24].

Using the effective Hamiltonian with 48 adjustable parameters we were able to reach the values $\chi_{GIP} = 2.13$ and $RMS_{GIP} = 0.00106\ cm^{-1}$. These values are close to χ_{RITZ} and RMS_{RITZ}, respectively. This means that the effective Hamiltonian model is adequate to data in a sense that it can reproduce the observed line positions with the accuracy close to the experimental uncertainties. The set of fitted effective Hamiltonian parameters is given in Table 5. The fit statistics for each band and for

each experimental source is presented in Tables 6 and 4, respectively.

5. Comparison with the HITRAN and the GEISA databases

The fitted set of parameters of the effective Hamiltonian for $^{16}O^{13}C^{18}O$ allowed us to generate the file of calculated line positions, which will be included in the future atmospheric [26] and high-temperature [27] versions of the Carbon Dioxide Spectroscopic Databank (CDSD). In this section we compare observed wavenumbers for $^{16}O^{13}C^{18}O$ with those contained in HI-

TRAN [23]. Since HITRAN and GEISA [28] databases contain identical $^{16}O^{13}C^{18}O$ data we shall consider HITRAN only. Before performing the comparison we give a brief analysis of $^{16}O^{13}C^{18}O$ data contained in the HITRAN database. The $^{16}O^{13}C^{18}O$ portion of the HITRAN database contains 2312 lines belonging to 17 bands covering the 567–4947 cm^{-1} spectral range. Only the lines with the intensities higher than 10^{-27} cm^{-1}/molecule cm^{-2} at 296 K have been included. It is known that no direct observations are used to generate HITRAN data for the carbon dioxide molecule. The molecular constants to generate these data are given in the paper of Rothman et al. [1]. Tables 1 and 2 of that paper give all needed information about the origin of the line

Table 6
Experimental data and statistics of the line positions fit for $^{16}O^{13}C^{18}O$ (band-by-band analysis)

$P' \rightarrow P$		$V' \rightarrow V$		J_{max}	N_{lin}	RMS	References
1	0	01101	00001	90	343	0.66	d,e
2	0	10001	00001	37	29	0.23	f
2	0	10002	00001	29	17	0.35	f
2	1	10001	01101	73	247	0.71	d,e
2	1	10002	01101	51	126	0.91	d,e
2	1	02201	01101	79	332	1.02	d,e
3	0	00011	00001	107	376	0.65	a,c,j
3	0	11101	00001	37	14	1.43	c,h
3	2	00011	10001	54	127	1.02	d,i
3	2	00011	10002	53	121	0.81	d,i
4	0	20002	00001	32	19	1.38	g
4	1	01111	01101	102	377	1.13	j,c
5	0	10011	00001	32	8	1.43	b
5	0	10012	00001	45	23	2.27	b
5	2	02211	02201	67	157	2.21	c
5	2	10011	10001	83	79	1.37	c
5	2	10012	10002	85	84	1.04	c
6	0	00021	00001	58	114	0.52	l
6	3	00021	00011	58	61	0.20	j
7	0	20011	00001	51	106	0.60	k,l
7	0	20012	00001	65	134	1.03	k,l
7	0	20013	00001	59	124	1.23	k,l
7	1	01121	01101	37	49	1.06	l
7	4	01121	01111	54	116	0.43	j
8	0	10021	00001	38	64	2.08	l
8	0	10022	00001	36	46	1.60	l
8	1	21112	01101	45	127	0.89	l
8	1	21113	01101	39	123	1.66	l
9	0	00031	00001	58	87	0.74	l
9	0	30011	00001	37	36	2.13	l
9	0	30012	00001	47	84	0.75	l
9	0	30013	00001	46	113	1.11	k,l
9	6	00031	00021	67	57	0.33	j
11	0	10031	00001	39	48	2.18	l
12	9	00041	00031	55	44	0.37	j
15	12	00051	00041	60	78	0.36	j
18	15	00061	00051	59	52	0.49	j
21	18	00071	00061	54	46	0.69	j
Total				107	4188	1.06	

P' and P are numbers of upper and lower polyad; V' and V are upper and lower vibrational states according to HITRAN notation; J_{max} is the maximum value of the rotational quantum number in the file of experimental data for a given band; N_{lin} is the total number of lines in the file of the experimental data for a given band; RMS (in 10^{-3} cm^{-1}) is the root-mean-square deviation for a given band. References: a—[2], b—[3], c—[4–7], d—[8], e—[9], f—[10], g—[11], h—[12], i—[13], j—[14], k—[17], l—this work.
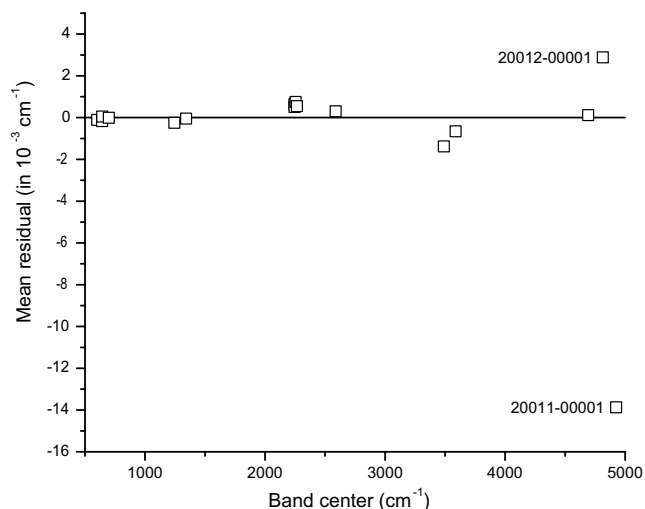
Fig. 3. Comparison of HITRAN with observed line positions. Two bands, 20011–00001 and 20012-00001, which have rather large values of MR (mean residual) are indicated explicitly.

parameters. An important indicator of the reliability of the line parameters is the IERR code, which contains the accuracy indices for frequency, intensity, and air-broadening halfwidth. The meaning of the IERR values is given at the end of the file "Table_97.txt" supplied with HITRAN. All lines higher than $4673\,cm^{-1}$ have 0 as the accuracy index for the line positions. All other lines have $IERR = 4$. It is possible to compare lines, which are present both in HITRAN and in observed datafile. For comparison it is convenient to use mean residual (MR) defined as

$$MR = \frac{1}{N} \sum_{i=1}^{N} (v_i^{obs} - v_i^{HITRAN}),\tag{8}$$

where N is the number of observed lines of a given band, v_i^{obs} and v_i^{HITRAN} are observed and HITRAN line positions, respectively. These MR versus band origins are given in Fig. 3. There are two bands, 20011–00001 and 20012–00001, which have rather large values of MR reaching $0.014\,cm^{-1}$. Because the line positions for the two bands listed in HITRAN were derived from the calculations of Chedin and Teffo [29] in 1984, so it is not surprising to see the differences between the present work and HITRAN database due to the limitations of the theoretical technique at that time. In fact they are within the uncertainties declared by these earlier works.

6. Conclusion

In the present paper Fourier-transform study of carbon dioxide isotope, $^{16}O^{13}C^{18}O$, was carried out in $4000–9500\,cm^{-1}$ region. Among the 14 bands rotational analyzed, eight of them are new while the rotational analysis of six others is improved. The new observations

together with data collected from the literature have been used to fit parameters of an effective Hamiltonian. The obtained set of 58 parameters (10 fixed and 48 adjustable) reproduces the observed dataset consisting of 4188 line positions of 38 bands with $RMS = 0.001\,cm^{-1}$. The results obtained in this paper will be used to extend the data contained in Carbon Dioxide Spectroscopic Databank (CDSD) located at the site http://cdsd.iao.ru.

References

[1] L.S. Rothman, R.L. Hawkins, R.B. Wattson, R.R. Gamache, J. Quant. Spectrosc. Radiat. Transfer 48 (1992) 537–566.
[2] A. Baldacci, L. Linden, V. Malathy Devi, K.N. Rao, B. Fridovich, J. Mol. Spectrosc. 72 (1978) 135–142.
[3] A. Baldacci, C.P. Rinsland, M.A.H. Smith, K.N. Rao, J. Mol. Spectrosc. 94 (1982) 351–362.
[4] M.P. Esplin, R.J. Huppi, G.A. Vanasse, Appl. Opt. 21 (1982) 1681–1685.
[5] M.P. Esplin, L.S. Rothman, J. Mol. Spectrosc. 100 (1983) 193–204.
[6] M.P. Esplin, L.S. Rothman, J. Mol. Spectrosc. 116 (1986) 351–363.
[7] M.P. Esplin, H. Sakai, L.S. Rothman, G.A. Vanasse, W. Barowy, R. Huppi, AFGL-TR-0046, 1986.
[8] M.P. Esplin, M.L. Hoke, in: High Resolution Fourier Transform Spectroscopy Technical Digest, Optical Society of America, Washington, DC, 1992, pp. 78–80.
[9] K. Jolma, J. Mol. Spectrosc. 111 (1985) 211–218.
[10] R.A. Toth, Appl. Opt. 24 (1985) 261–274.
[11] V. Malathy Devi, C.P. Rinsland, D.C. Benner, Appl. Opt. 23 (1984) 4067–4075.
[12] C.P. Rinsland, D.C. Benner, V. Malathy Devi, Appl. Opt. 24 (1985) 1644–1650.
[13] L.C. Bradley, K.L. Soohoo, C. Freed, IEEE J. Quantum Electron. 22 (1986) 234–267.
[14] D. Bailly, C. Rossetti, J. Mol. Spectrosc. 119 (1986) 388–397.
[15] J. Connes, P. Connes, J.-P. Maillard, Altas des spectres dans le proche infrarouge de Vénus, Mars, Jupiter et Saturne, CNRS, Paris, 1969.
[16] P. Connes, G. Michel, Astrophys. J. Lett. Ed. 190 (1974) L24.
[17] J.-Y. Mandin, J. Mol. Spectrosc. 67 (1977) 304–321.
[18] C. Miller, private communication, Haverford College, USA, 2002.
[19] J.-L. Teffo, O.N. Sulakshina, V.I. Perevalov, J. Mol. Spectrosc. 156 (1992) 48–64.

[20] S.A. Tashkun, V.I. Perevalov, J.-L. Teffo, L.S. Rothman, Vl.G. Tyuterev, J. Quant. Spectrosc. Radiat. Transfer 60 (1998) 785–801.

[21] S.A. Tashkun, V.I. Perevalov, J.-L. Teffo, M. Lecoutre, T.R. Huet, A. Campargue, D. Bailly, M.P. Esplin, J. Mol. Spectrosc. 200 (2000) 162–176.

[22] S.A. Tashkun, V.I. Perevalov, J.-L. Teffo, J. Mol. Spectrosc. 201 (2001) 137–145.

[23] L.S. Rothman, C.P. Rinsland, A. Goldman, S.T. Massie, D.P. Edwards, J.-M. Flaud, A. Perrin, C. Camy-Peyret, V. Dana, J.-Y. Mandin, J. Schroeder, A. McCann, R.R. Gamache, R.B. Wattson, K. Yoshino, K.V. Chance, K.W. Jucks, L.R. Brown, V. Nemtchinov, P. Varanasi, J. Quant. Spectrosc. Radiat. Transfer 60 (1998) 665–710.

[24] A. Chédin, J. Mol. Spectrosc. 76 (1979) 430–491.

[25] S.A. Tashkun, V.G. Tyuterev, in: A.I. Nadezhdinskii, Y.N. Ponomarev, L.N. Sinitsa (Eds.), Proceedings of the 11th Symposium and School on High-Resolution Molecular Spectroscopy, SPIE, 2205, 1993, pp. 188–191.

[26] S.A. Tashkun, V.I. Perevalov, J.-L. Teffo, HITRAN Database Conference, 25th Anniversary of HITRAN, AFRL/VS-East Science Center, 1998, p. 5.

[27] S.A. Tashkun, V.I. Perevalov, J.-L. Teffo, A.D. Bykov, N.N. Lavrentieva, J. Quant. Spectrosc. Radiat. Transfer 82 (2003) 165–196.

[28] N. Jacquinet-Husson, E. Arié, J. Ballard, A. Barbe, G. Bjoraker, B. Bonnet, L.R. Brown, C. Camy-Peyret, J.P. Champion, A. Chédin, A. Chursin, C. Clerbaux, G. Duxbury, J.-M. Flaud, N. Fourrié, A. Fayt, G. Graner, R. Gamache, A. Goldman, Vl. Golovko, G. Guelachvili, J.M. Hartmann, J.C. Hilico, J. Hillman, G. Lefèvre, E. Lellouch, S.N. Mikhailenko, O.V. Naumenko, V. Nemtchinov, D.A. Newnham, A. Nikitin, J. Orphal, A. Perrin, D.C. Reuter, C.P. Rinsland, L. Rosenmann, L.S. Rothman, N.A. Scott, J. Selby, L.N. Sinitsa, J.M. Sirota, A.M. Smith, K.M. Smith, Vl. G. Tyuterev, R.H. Tipping, S. Urban, P. Varanasi, M. Weber, J. Quant. Spectrosc. Radiat. Transfer 62 (1999) 205–253.

[29] A. Chedin, J.-L. Teffo, J. Mol. Spectrosc. 107 (1984) 333–342.